International Journal of Mechanical and Electrical Engineering
ISSN: 3005-9615 (Print), ISSN: 3005-7132 (Online) | Volume 2, Number 1, Year 2024
DOI: https://doi.org/10.62051/ijmee.v2n1.13
Journal homepage: https://wepub.org/index.php/IJMEE/index

Preparation and Performance Study of Alkali-active Gypsum Mixture System

Mifeng Gou *, Xiangquan Yang, Mengdan Zhang

School of Materials Science and Engineering, Henan Polytechnic University, Jiaozuo Henan, 454000, China

* Corresponding Author: Mifeng Gou

ABSTRACT

To improve the mechanical properties and water resistance of gypsum specimens, thus solving the pollution problem due to the accumulation of flue gas desulfurization gypsum (FGD gypsum), etc. The article utilizes flue gas desulfurization gypsum, gypsum citrate, and mineral powder as the main raw materials under a fixed ratio. The Alkali-activation gypsum-based cementitious material (Alkali-activation GM-S95 system) was obtained by modifying it with 0-5% Na(OH) and Ca(OH)2 alkaline admixtures, and the mechanical properties and water resistance of the Alkali-activation GM-S95 system were thoroughly investigated. The structural characteristics of the Alkali-activation GM-S95 system specimens were investigated using XRD, TG, SEM and LF-NMR techniques to explore their interactions. The results showed that the compressive strength of the Alkali-activation GM-S95 system was significantly increased to 26 MPa when 4% Ca(OH)2 was added alone, and the water absorption was decreased to 12.5%.The addition of 4% Ca(OH)2 caused the crystals of gypsum dihydrate to be thicker and denser, and AFT and C-S-H gels were produced, which were attached around the crystals of gypsum dihydrate. The addition of different admixtures can reduce the proportion of large pores and further fill the crystal structure. In summary, the addition of 4% Ca(OH)2 can improve the compressive strength and water resistance of the samples of Alkali-activation GM-S95 system, thus laying a solid foundation for the comprehensive utilization of flue gas desulfurization gypsum.

KEYWORDS

FGD Gypsum; Compressive Strength; Low-field Nuclear Magnetic Field; Ca (OH)2; Microstructure.

1. INTRODUCTION

Flue gas desulfurization gypsum (FGD) is an industrial by-product produced after industrial desulfurization treatment mainly gypsum dihydrate ($CaSO_4 \cdot 2H_2O$) [1], [2], [3], [4]. However, a large amount of FGD is piled up and shelved occupying a large amount of land resources, and its substances also cause secondary pollution to the natural environment [5], [6, 7], it is significant to improve the resource utilization of FGD and the sustainable development process of the material.

FGD gypsum is calcined and calcium sulfate dihydrate is burned into calcium sulfate hemihydrate, and the product has the characteristics of low carbon, light weight, refractory, etc. [8- 9 ,10 ,11], which can be mainly used in the production of plaster, paper-faced gypsum board, gypsum blocks, etc. [12]; but due to its pores and solubility of calcium sulfate dihydrate crystals, resulting in poor water resistance and mechanical properties, etc., it is easy to be destroyed under the condition of high humidity [13]. Therefore, it is important to improve such performance of FGD to increase its utilization.

In order to strengthen the resource utilization of industrial waste gypsum and building energy saving, to overcome the drawbacks of water resistance and mechanical properties many scholars have found an effective way in their research [14, 15, 16, 17, 18, 19] this paper investigates the effects of different ratios of Na(OH) and $Ca(OH)_2$ chemical admixtures on the mechanical properties of Alkali-activation gypsum mixture system and water resistance, etc., and explores the effects of the two different kinds of chemical admixtures Na(OH) and $Ca(OH)_2$ on the macroscopic property changes of Alkali-activation gypsum mixture system. chemical admixtures on the macroscopic property changes of Alkali-activation gypsum mixture systems. TG-DTG, XRD and SEM were used to analyze and study the system changes.

2. MATERIALS AND METHODS

2.1. Raw Materials

The building gypsum for desulfurization (FGD) used in this paper was purchased from Henan Gaisen Materials Technology Co.(Jiaozuo,China). The physical phase composition and microstructure of gypsum are shown in Fig. 1. Its main crystalline phase is hemihydrate gypsum (CaSO4·0.5H2O). The specific surface area was 380 m2 / kg.

Mineral powder (S95) was produced by Gongyi Longze Water Purification Materials Co. The water content was 0.45 % and the specific surface area was 429 m2 / kg. Figure 3 shows that the mineral composition of the mineral powder was mainly vitreous. The chemical composition of the main materials is shown in Table 1 and Figure 3 shows the particle size distribution of the main materials. The median particle sizes of desulfurization gypsum, citrate gypsum, and mineral powder were 28.8 μm, 7.97 μm, and 14.6 μm, respectively.

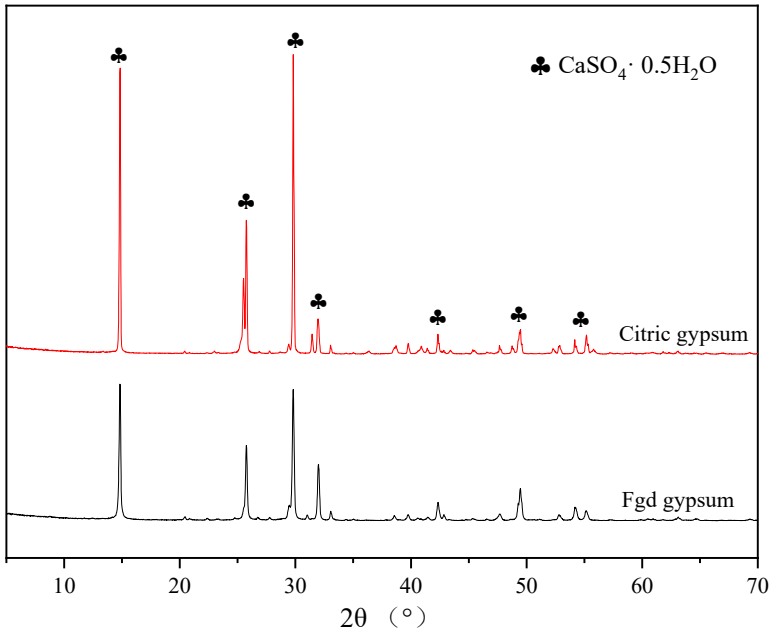

Figure 1. FGD gypsum and Gypsum citrate XRD

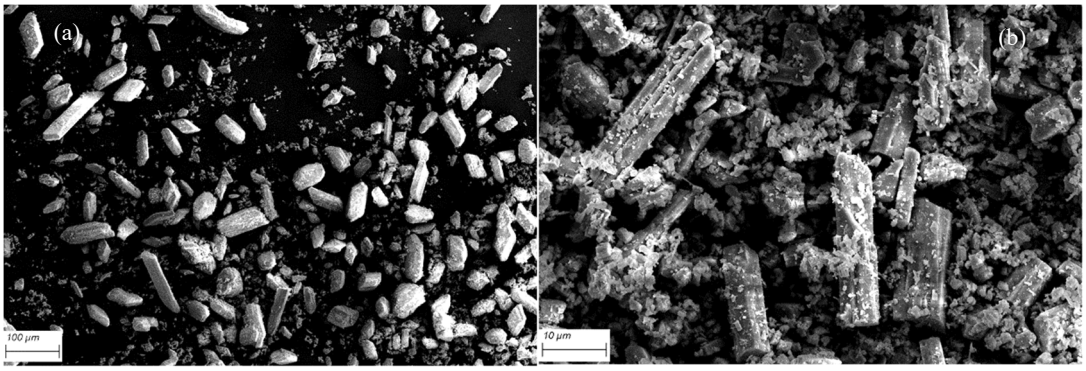

Figure 2. FGD gypsum (a) and Gypsum citrate (b) SEM

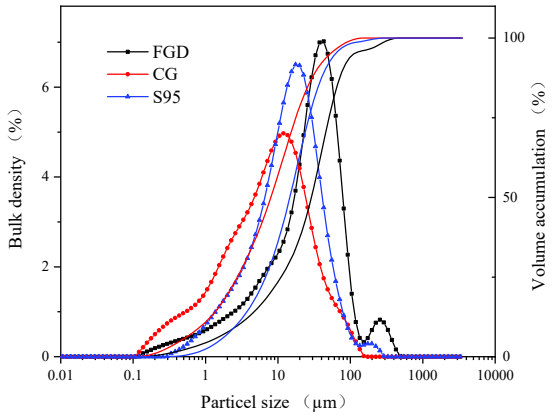

Figure 3. Raw material particle size

Table 1. Chemical compositions of main materials(wt/%).

Compositions	SiO_2	CaO	Al_2O_3	Fe_2O_3	MgO	SO_3
Gypsum	4.30	31.97	3.10	0.33	0.18	51.84
Gypsum citrate	0.26	40.85	0.17	0.09	0.12	58.37
Mineral powder	34.50	34.00	17.70	1.03	6.01	1.64

2.2. Mix Proportions and Research Framework

2.2.1. Experimental Design

Two alkaline admixtures, Na(OH) and Ca(OH)2 (0%-5%), were used for the investigation, in which the water-cement ratio was determined to be 0.52 and the gypsum mix was GM-S95,which is mainly a mixture of 10% mineral powder, 15% gypsum citrate and 85% FGD gypsum. The specific test mixes are shown in Table 2.

2.2.2. Preparation of Test Samples

After weighing each of the above mentioned materials and using a net slurry mixer, water was added and mixed for 2 min to obtain a homogeneous mixture. The homogeneous slurry was quickly poured into the mold. 24 h later the mold was demolded and cured at room temperature of 24±2°C until age for different performance tests.

Table 2. Alkali-active gypsum base cementitious system (wt)

Samples	gypsum	Mineral powder	$Na(OH)/Ca(OH)_2$
0	630	70	0
1N	630	70	7
2N	630	70	14
3N	630	70	21
4N	630	70	28
5N	630	70	35
1C	630	70	7
2C	630	70	14
3C	630	70	21
4C	630	70	28
5C	630	70	35

2.3. Methods

2.3.1. Physical Properties

Compressive strength test is performed in accordance with GB / T 17669.3 - 1999 to determine the compressive and flexural strength.

2.3.2. Softening Coefficient and Water Absorption

Determine the softening coefficient of the specimen according to JC / T698 - 2010.

2.3.3. TG-DTA

Beijing Hengjiu Scientific Instrument Factory BJ-HCT-3 comprehensive thermal analyzer was used for the analysis.

2.3.4. Low Field Nuclear Magnetic Resonance

The pore structure analysis was carried out using a (MesoMR12-060V) microstructure test analyzer from Suzhou Newmax Analytical Instruments Co.

2.3.5. Microstructure Tests

The samples to be tested were soaked in anhydrous ethanol and dried, then ground in an agate mortar until the particle fineness was less than 40 μm, and analyzed for mineralogical composition using a Smart - Lab X-ray diffractometer (XRD , Rigaku , Smartlab , Tokyo , Japan).

A Merlin Compact scanning electron microscope (Carl Zeiss NTS GmbH, Germany) was used to analyze the specimens for micro-morphological observation.

3. RESULTS AND DISCUSSION

3.1. Compressive Strength

The compressive strength of Alkali-activation GC-S95 system with different proportions of Na(OH) and Ca(OH)2 added to gypsum mixture is shown in Fig. 4. With the addition of different dosages of Na(OH) and Ca(OH)2, the mechanical properties of Alkali-activation GC-S95 system showed different trends, and the Na(OH) brought about a different degree of decrease in the gypsum mixture, on the contrary, the addition of Ca(OH)2 improved the mechanical properties of Alkali-activation GC-S95 system at different degrees.increased the mechanical properties of Alkali-activation GC-S95 system to different degrees. The compressive resistance of Alkali-activation GC-S95 system with different amounts of Na(OH) increased from 14.9 MPa to 16.4 MPa only at 3d and 1% addition, but decreased all the way down to 3.07 MPa at 5% with gradual increase of Na(OH), and also decreased from 22.9 MPa and 17.8 MPa to 6.27 MPa and 4.90 MPa at 14d and 28d. However, the addition of different amounts of Ca(OH)2 brought an enhancement to the gypsum mixture, increasing the compressive strength from 14.9 MPa to 19.2 MPa at 3 d, and also from 22.9 MPa, 17.8 MPa to 26 MPa, 19.1 MPa at 14 d. The results indicated that Na(OH) acted in the opposite direction on the performance of the Alkali-activation GC-S95 system, and Na (OH) addition decreased the mechanical properties of Alkali-activation GC-S95 system, which was mainly due to the excessive alkaline admixture affecting the hydration of gypsum dihydrate and propping up the structure. On the other hand, Ca(OH)2 has not obvious enough to improve the performance of Alkali-activation GC-S95 system, which proves that the addition of 4% dosage of Ca(OH)2 promotes the mineral powder and gypsum crystals together and improves the performance of Alkali-activation GC-S95 system.

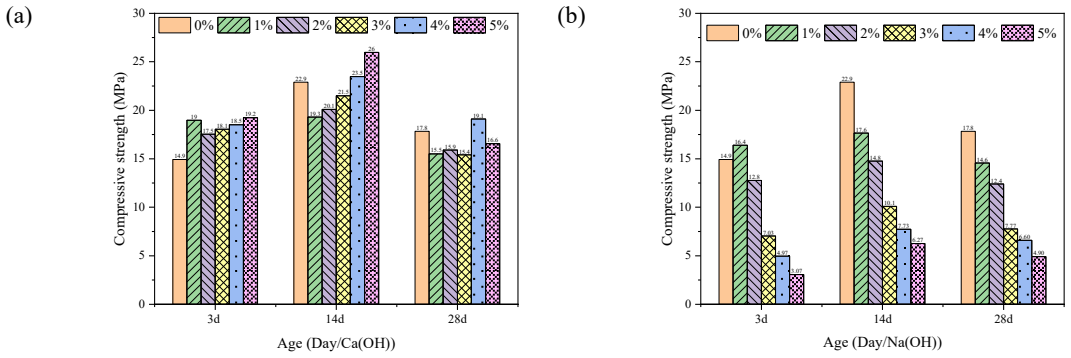

Figure 4. Compressive strength of Ca(OH)(a) and Na(OH) (b) content

3.2. Water Resistance

The water absorption of Alkali-activation GC-S95 system with the addition of different proportions of Na(OH) and Ca(OH)2 to the gypsum mix is shown in Figure 5. With the addition of different dosages of Na(OH) and Ca(OH)2, the water absorption of Alkali-activation GC-S95 system showed different degrees of decreases, at the lowest close to 12.5%. with different dosages of Ca(OH)2, the water absorption decreased from 20.5% and 18.6% to 17.1% and 16.2% for 3d and 28d, respectively, and tended to slow down at 3% Ca(OH)2 and reached a lower value of 16.2% at 4% Ca(OH)2; however, when Na(OH) was added, the 3d water absorption showed a significant decrease after 2% Na(OH) to 12.8% at 5% Na(OH), and the 28d water absorption showed a slow tendency to decrease down to a minimum of 16.2%. The water resistance of Alkali-activation GC-S95 system was improved by different alkaline admixtures, which is mainly due to the alkaline material's water resistance, which protects the overall material.

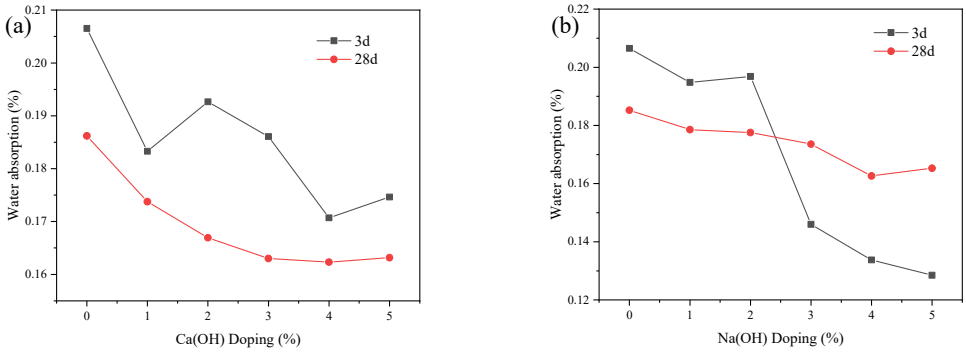

Figure 5. Water absorption of Ca(OH)(a) and Na(OH) (b) content

3.3. XRD Analysis

Figure 6 analyzes the hydration products in the Alkali-activation GC-S95 architecture. Results. Some of the improved properties in the Alkali-activation GC-S95 system are hydration products under alkaline conditions.The XRD spectra show that the main peaks observed in the samples are from the formation of gypsum dihydrate (CaSO4-2H2O) by the hydration process of gypsum hemihydrate (CaSO4-0.5H2O) in the GM as well as from some of the unhydrated gypsum hemihydrate. The main peaks of the Alkali-activation GC-S95 system changed to different degrees after GM-S95 and different doping amounts of Na(OH) and Ca(OH)2, and the peak heights were all increased. This is mainly due to the fact that a large amount of CH produced during the hydration reaction in Na(OH) and Ca(OH)2 formed an alkaline environment at the same time, which produced an alkaline excitation effect on the mineral powders in the alkaline-excited GC-S95 system. This effect enhanced the reactivity of Al2O32-, SiO32- and other components of the mineral powder with gypsum in the Alkali-activation GC-S95 system, resulting in the generation of C-S-H gels and Aft.As a result, CH will be consumed in large quantities, leading to a decrease in its concentration and thus promoting the formation of gypsum dihydrate (CaSO4-2H2O). However, due to the limited addition of S95 , Na(OH) and Ca(OH)2 to the Alkali-activation GC-S95 system, the C-S-H gels and calcium aluminate (Aft) peaks generated by the Alkali-activation GC-S95 system are not obvious, but change part of the gypsum crystalline shape. This suggests that 4% Ca(OH)2 addition has a significant effect on the enhancement of mechanical properties and water resistance of the Alkali-activation GC-S95 system with low mineral powder content[20].

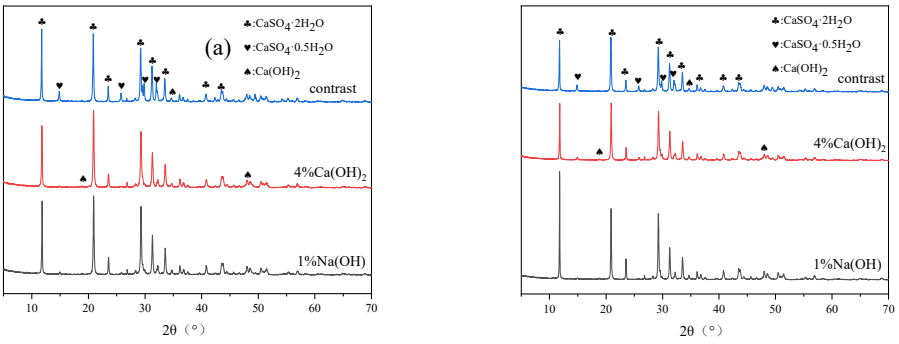

Figure 6. XRD pattern of alkali active system. (a)3d (b)14d.

3.4. Thermal Analysis

Figure 7 shows the TG analysis results and mass loss curves of the Alkali-activation GC-S95 system. The heat absorption peaks of the Alkali-activation GC-S95 system observed in the figure at

110~195°C are due to the dehydration of water molecules in the crystal structure of gypsum dihydrate. In contrast to this phenomenon, the TG curve for 0 shows a mass loss of 15.29%, 1N a mass loss of about 16.91% and 4C a mass loss of about 15.79%. In the temperature range of 55 - 110°C, the TG curves for 1N and 4C show insignificant mass loss of 1.36% and 1.67%, respectively. The corresponding DTG heat absorption peaks are attributed to the overlapping effects of calomel, C-S-H gel and free water in the Alkali-activation GC-S95 system. In contrast, the weak heat absorption peak near 650°C in the Alkali-activation GC-S95 system is attributed to the decomposition of hydroxycalcite (Ca(OH)2) and calcite (CaCO3). A small amount of calcite and C-S-H gel were formed in the Alkali-activation GC-S95 system, and the hydration products were relatively small and inconspicuous due to the low S95 content. This indicates that a small amount of mineral powder in 4% Ca(OH)2 alkaline excitation under the gelling activity of the better effect.

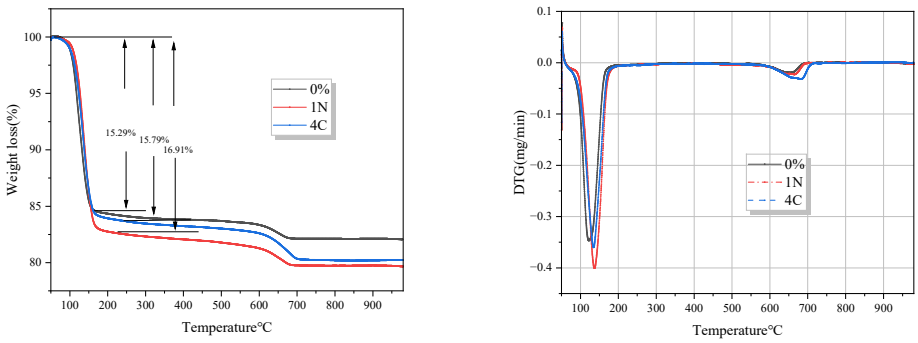

Figure 7. TG and DTG curves of alkali active system

3.5. LF-NMR Analysis

The low-field NMR pore structures of Alkali-activation GC-S95 system are shown in Figs.8 and 9. The T2 main peak of the Alkali-activation GC-S95 system appears at 2.5-45ms with different additions of Na(OH) and $Ca(OH)_2$, and the relaxation time main peak region is still in the range of 2.5-45ms with the increase of age. However, with the changes of Na(OH) and $Ca(OH)_2$, the T2 main peak of the Alkali-activation GC-S95 system was the lowest at 4C, and the pore size of the Alkali-activation GC-S95 system underwent a transition from polyhazardous to hazardous pores. In the case of 4% Ca(OH), the total pore volume was less than that of the blank group at 3d and 28d, decreasing from 27.18% and 23.69% to 24.98% and 22.01%, respectively, and the percentage of gelatinous pores and less-harmful pores reached 3.99% and 8.34% at 3d, which were higher than that of the blank group at 1.77% and 5.83%. The number of multi-hazardous holes was less than that of the blank group, from 19.6% to 12.7%.The percentage of gelatinized holes and less-hazardous holes reached 3.10% and 6.39% at 28d, which were still higher than that of the blank group (1.88% and 6.09%), and the number of multi-hazardous holes was less than that of the blank group (from 15.7% to 12.5%).

In the case of 1% NaOH, the proportion of gelled pores and less harmful pores were 9.22% and 4.79% at 3d, which were higher than 1.77% and 5.83% in the blank group, while the proportion was only 1.85% and 3.89% at 28d, which were lower than 1.88% and 6.09% in the blank group. The percentage of multi-hazardous pores at 3d was 12.7%, lower than that of 19.6% in the blank group, and at 28d was 21.2%, much more than that of 15.7% in the blank group. the pore structure at 3d was better than that of the blank group, revealing that the 3d strength was greater than that of the blank group. And the poor pore structure at 28d and the corresponding decrease in strength proved that more free water pores existed in the non-harmful pores and gel pores at the initial stage rather than gel pores, which further expanded and evolved into harmful pores and multi-harmful pores at the later stage. In contrast, at 4C, the number of polyhazardous pores was significantly reduced, and the proportion of non-hazardous pores and gel pores continued to increase, which improved the inter-crystalline structure density and stability of the Alkali-activation GC-S95 system [10]. In addition, the analysis of pore

size distribution confirmed that the addition of 4% $Ca(OH)_2$ had an enhancement effect on the mechanical properties and water resistance of the Alkali-activation GC-S95 system [20].

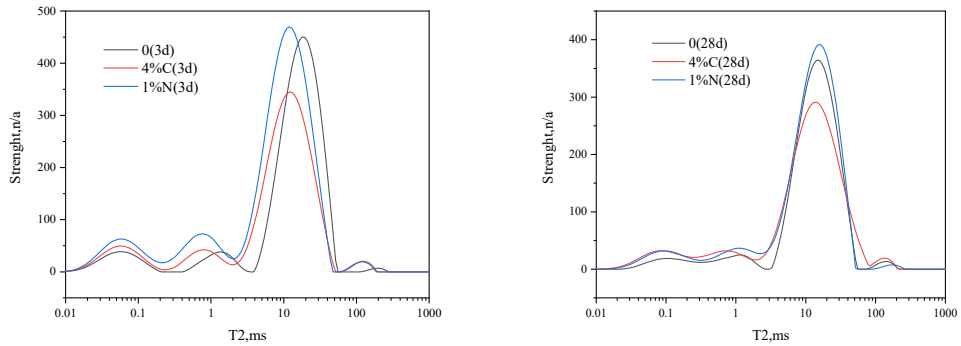

Figure 8. T2 relaxation signals of Alkali-active system

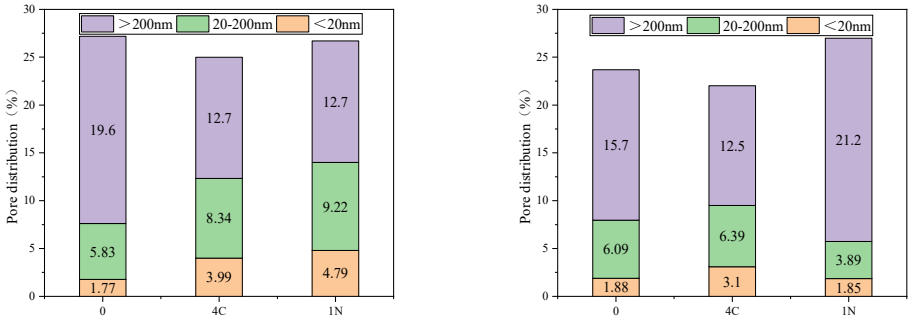

Figure 9. Pore size distribution of Alkali-active system

3.6. SEM Analysis

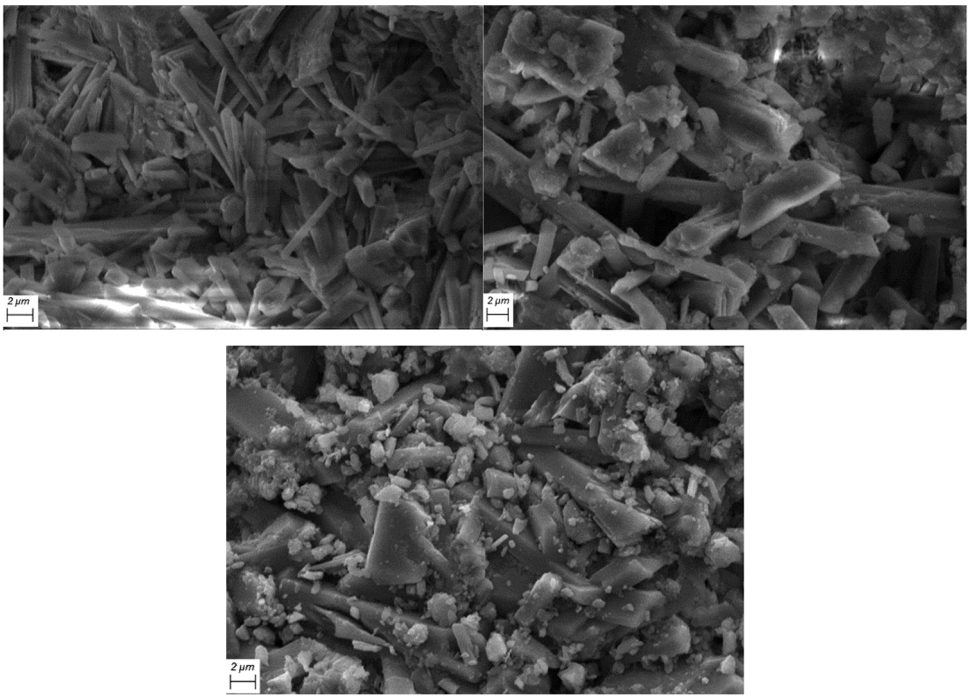

Figure 10. SEM images of Alkali-active system (a) 0, (b)1N, (c)4C

Figures 10 show the microscopic morphology of the Alkali-activation GC-S95 system with the addition of different Na(OH) and $Ca(OH)_2$. The Alkali-activation GC-S95 system has a loosely packed columnar or lamellar crystal structure in 0, with obvious gaps. However, upon addition of different Na(OH) and $Ca(OH)_2$, it can be seen that different reactions occur due to C-S-H gel attachment to the surface of calcium sulfate dihydrate crystals, but with different alkaline admixtures. In the 1N of the Alkali-activation GC-S95 system with the addition of Na(OH), the presence of C-S-H gel between the crystals makes the gypsum dihydrate crystals connected, but also brings more pores; while in the Alkali-activation GC-S95 system with the addition of $Ca(OH)_2$, the presence of C-S-H gel between the crystals is still obvious making the gypsum dihydrate crystals tightly connected with fewer pores. C-S-H gels and other substances on the 4C Alkali-activation GC-S95 system of gypsum dihydrate ($CaSO_4$-$2H_2O$) crystals have a wrapping effect at the same time, they can also fill the 4C structure of gypsum dihydrate crystals of the gaps between the Alkali-activation GC-S95 system through the cementation effect enhances the stability, densification. Therefore, the 4% doping of $Ca(OH)_2$ case favors the formation of C-S-H, which contributes to the enhancement of the dense filling efficiency of Alkali-activation GC-S95 system and correspondingly improves the mechanical properties and water resistance of Alkali-activation GC-S95 system [21].

4. CONCLUSION

Different alkaline admixtures Na(OH) and $Ca(OH)_2$ doped into the GC-mineral powder system, to alkaline-excited GC-S95 system, different reactions occurred and produced different effects.

(1) Different Na(OH) and $Ca(OH)_2$ were doped into the GC-mineral powder system, and the strength of the Alkali-activation GC-S95 system decreased under the action of different dosages of Na(OH), which brought negative effects on the system; the mechanical properties of the Alkali-activation GC-S95 system grew at different stages under the action of 4% $Ca(OH)_2$.

(2) Different Na(OH) and $Ca(OH)_2$ were added to the GC-mineral powder system, and by analyzing the effects of the interactions between the components on the water resistance, it was concluded that the different alkaline admixtures all had an enhancement effect on the water resistance of Alkali-activation GC-S95 system, and the water absorption decreased to about 12.7% at the lowest stage, and the softening coefficient increased to about 0.87. Different alkaline admixtures improved the water resistance of alkaline-excited GC-S95 system.

(3) By analyzing the microscopic morphology and pore size distribution of alkaline-excited GC-S95 system, the alkaline-excited GC-S95 system under the action of 4% $Ca(OH)_2$, the distribution of harmful pores and polyhazardous pores were reduced, and the harmless pores and gelatinized pores were increased; in terms of microscopic morphology, there was more compactness between the crystalline structures, and there were fewer pores.The doping amount of 4% $Ca(OH)_2$ has a better The effect of 4% $Ca(OH)_2$ doping on the Alkali-activation GC-S95 system is better.

5. CONFLICTS OF INTEREST

The authors have indicated that they have no known competing financial interests or personal relationships that may have influenced the work reported in this paper.

ACKNOWLEDGMENTS

The authors gratefully acknowledge the Science and Technology Project of Henan Province (232102321145) and the Key Public Welfare Special Project of Henan Province (201300311000).

REFERENCES

[1] C. Li, L. Jiang, Effect of flue gas desulfurization gypsum addition on critical chloride content for rebar corrosion in fly ash concrete, Constr. Build. Mater. 286 (2021), https://doi.org/10.1016/j.conbuildmat.

[2] H. Fu, J. Huang, et al., Retard-ing e ect of impurities on the transformation kinetics of FGD gypsum to alpha-calcium sulfate hemihydrate under atmospheric and hydrothermal conditions. Fuel 203:445–451. https:// doi.org/ 10. 1016/j. fuel.

[3] K. Wang, Orndor W, et al., Mercury transportation in soil via using gypsum from flue gas desulfurization unit in coal-fired power plant. J Environ Sci 25(9):1858–1864. https://doi.org/ 10.1 016/s 1001- 0742(12) 60265-4

[4] J. Zhang, S. Li, Z. Li, Investigation the synergistic effects in quaternary binder containing red mud, blast furnace slag, steel slag and flue gas desulfurization gypsum based on artificial neural networks, J. Clean. Prod. 273 (2020), 122972, https://doi.org/10.1016/j.jclepro.

[5] A. Ahmed, K. Ugai, Environmental effects on durability of soil stabilized with recycled gypsum, Cold Reg. Sci.Technol.662–3(2011)84–92.

[6] A. Ahmed, U. H. Issa, Stability of soft clay soil stabilised with recycled gypsum in a wet environment, Soils Found.543(2014)405–416.

[7] Fu B, Liu GJ, Mian MM, Sun M, Wu D (2019) Characteristics and speciation of heavy metals in fly ash and FGD gypsum from Chi-nese coal-fired power plants. Fuel 251:593–602. https:// doi. org/ 10.1 016/j.f uel.

[8] G. Vasconcelos, P.B. Lourenço, A. Camo˜es, A. Martins, S. Cunha, Evaluation of the performance of recycled textile fibres in the mechanical behaviour of a gypsum and cork composite material, Cem. Concr. Compos. 58 (2015) 29–39, https://doi.org/ 10.1016/j.cemconcomp.

[9] C. Xu, W. Ni, K. Li, S. Zhang, D. Xu, Activation mechanisms of three types of industrial by-product gypsums on steel slag–granulated blast furnace slag-based binders, Constr. Build. Mater. 288 (2021), https://doi.org/10.1016/j. conbuildmat..

[10] A. Ahmed, K. Ugai, T. Kamei, Investigation of recycled gypsum in conjunction with waste plastic trays for ground improvement, Construct. Build. Mater. 251(2011)208–217.

[11] T. Kamei, A. Ahmed, K. Ugai, Durability of soft clay soil stabilized with recycled Bassanite and furnace cement mixtures, Soils Found.531(2013)155–165.

[12] T.D. Nguyen, J. Ambroise, Contribution of calcium aluminates to the water resistance of hydrated calcium sulfates, IOP Conf. Ser. Mater. Sci. Eng. (2020), https://doi.org/10.1088/1757-899x/869/3/032051.

[13] A. Rahmati, M. Gholamian, et al., An efficient model for estimation of gypsum (calcium sulfate di-hydrate) solubility in aqueous electrolyte solutions over wide temperature ranges, J. Mol. Liq. 281 (2019) 655–670, https:// doi.org/ 10.1016/j. molliq.

[14] G. Camarini, J.A. De Milito, Gypsum hemihydrate–cement blends to improve renderings durability, Construct. Build. Mater.2511(2011)4121–4125

[15] M. Arikan, K. Sobolev, The optimization of a gypsum-based composite material, Cement Concr. Res. 3211 (2002) 1725–1728.

[16] F.-q. Zhao, H.-j. Liu, L.-x. Hao, et al., Water resistant block from desulfurization gypsum, Construct. Build.Mater.271(2012)531–533.

[17] R. X. Magallanes-Rivera, J.I. Escalante-García, Hemihydrate or waste anhydrite in composite binders with blast-furnace slag: hydration products, microstructures and dimensional stability, Construct. Build. Mater.71(2014)317–326.

[18] M. Pang, Z. Sun, H. Huang, Compressive Strength and Durability of FGD Gypsum-Based Mortars Blended with Ground Granulated Blast Furnace Slag, Materials (Basel),2020, p.1315.

[19] P. C. Supaporn Wansom*,Wananurat Srijampan, Water resistant blended cements containing flue-gas desulfurization gypsum,Portland cement and fly ash forstructural applications,Cem.Concr.Compos.103(2019).

[20] Li Guangning. Research on the performance and application of alkali-excited gypsum composite cementitious materials [D]. Shandong University of Architecture,2023.

[21] Gou Bibo, Wang Haifeng et al. Influence of pretreatment pH of phosphogypsum on its preparation of no-bake cementitious materials[J]. New Building Materials,2022,49(01):13-17.